Chiral Poly(fluorene-alt-benzothiadiazole) (PFBT) and Nanocomposites with Gold Nanoparticles: Plasmonically and Structurally Enhanced Chirality

Heong Sub Oh, Sha Liu, HongSub Jee, Alexander Baev, Mark T. Swihart, and Paras N. Prasad*

Institute for Lasers, Photonics and Biophotonics, Department of Chemistry, Department of Chemical and Biological Engineering, and Department of Electrical Engineering, University at Buffalo, The State University of New York, Buffalo, New York 14260, United States

Received August 6, 2010; E-mail: pnprasad@buffalo.edu

Abstract: Materials with large chiral optical activity at visible wavelengths are of great interest in photonics, particularly as a route to chiral optical metamaterials. Here, we demonstrate the plasmonic enhancement of the chiral optical activity of chiral poly(fluorene-alt-benzothiadiazole) (PFBT) doped with gold nano-particles. The supramolecular helical organization of polymeric chains with simultaneous dipole−dipole interaction of the helically ordered nanoparticles with the polymer and one another results in unprecedented values of chirality parameter ($\kappa \sim 0.02$) at visible wavelengths in thin films.

Polyfluorenes[1,2] and their copolymers[3,4] are of great interest as π-conjugated conductive polymers and candidates for use in organic solar cells[5−8] and polymer light emitting diodes (PLEDs).[2,3,9−13] Interest in chiral structures has grown based on their potential use in enantioselective catalysis[14] and separation[15] and for optoelectronic applications.[16] Superstructures composed of nanoparticles and chiral molecules can serve as building blocks for optically active macromolecular complexes.[17] This enables new "bottom-up" approaches to optical metamaterials.[17,18] Although various synthetic protocols for inducing enantioselective interactions of nanoparticles with chiral molecules have been designed,[19] the physicochemical interactions between nanocrystals and supramolecular systems that can enhance chirality are complex and not yet fully understood. Electronic circular dichroism (CD) has been used to investigate chirality transfer in molecular systems, showing that chiral molecules can induce polarization-dependent optical activity in achiral (metal and semiconductor) nanoparticles.[20]

In particular, noble metal nanoparticles in close contact with chiral molecules have been shown to exhibit optical activity at their plasmonic frequencies.[20a,21] Such nanoparticles are generally capped (passivated) with small chiral ligands[20a,21] or grown on chiral templates.[22] In spite of significant progress in such systems, their absolute optical activity (e.g., chirality parameter, κ) is usually very low. Moreover, they are not suitable for film fabrication without addition of a matrix material. Chirality transfer from chiral polymers, as opposed to small chiral ligands, to nanomaterials is not well studied. Herein we report chiroptical properties of a newly synthesized chiral polymer, poly(fluorene-alt-benzothiadiazole) (PFBT) alone and with the addition of gold nanoparticles (AuNPs). Annealing of the polymer or nanocomposite induces ordering that leads to dramatic increases in optical activity. Optical activity of the annealed nanocomposite is further dramatically enhanced relative to the annealed polymer or unannealed nanocomposite. The overall process of nanocomposite formation and helical self-assembly during annealing is illustrated in schematically in Figure 1.
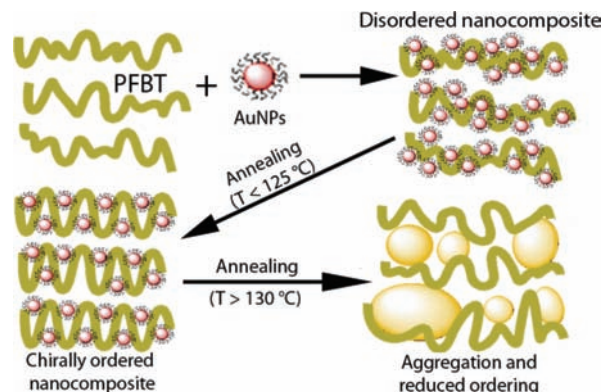

Figure 1. Schematic illustration of formation of helically ordered AuNP/PFBT nanocomposites with extraordinary optical activity.

We introduced chirality in PBFT by attaching (*S*)-3,7-dimethyloctyl substituents at the 9-positions of the fluorene monomer. Meijer et al.[23] reported that thermal annealing of a specific chiral PFBT molecular weight fraction induced an irreversible phase transition to a liquid crystalline state that vitrified upon cooling and exhibited considerable circular dichroism (CD). The CD response depended on the molecular weight, with an intermediate fraction (M_n, 5110) yielding the maximum CD signal. Here, we synthesized PFBT using palladium-catalyzed Suzuki polycondensation as the final step and purified the product with Soxhlet extraction[23] to obtain high molecular weight (M_n = 13 000, M_w = 30 000) PFBT. We confirmed its structure by ^{1}H NMR, GPC, and DSC (see Supporting Information). Films were prepared by spin-casting (~4 mg of PFBT in 1 mL of chloroform/chlorobenzene, 10/1, v/v), followed by annealing at 100 to 175 °C. The L-isomer of PFBT possesses strong absorption at 467 nm that decreased slightly with increased annealing temperature (Figure S3a). The corresponding CD band position showed a weak dependence on annealing temperature with a slight blue shift of the most intense peak from 472 to 468 nm. However the CD band intensity depended strongly on annealing temperature, increasing up to 125 °C and then gradually decreasing at higher temperature (Figure S3).

To produce AuNP/PFBT nanocomposites, ~4 nm dodecylamine capped or ~10 nm oleylamine capped AuNPs[24] (0.25 to 10 mg in 0.5 mL of chloroform/chlorobenzene, 10/1, v/v) were mixed with PFBT (4 mg of PFBT in 0.5 mL of chloroform/chlorobenzene, 10/1, v/v) at four different concentration ratios. The resulting dispersions were stable for several days. Films prepared by spin-coating onto a glass substrate were annealed at 100 to 175 °C. Incorporation of AuNPs into the AuNP/PFBT nanocomposite was confirmed by HRTEM, AFM, and SEM imaging. The addition of AuNPs led to a dramatic increase in the intensity of the CD band near 480 nm
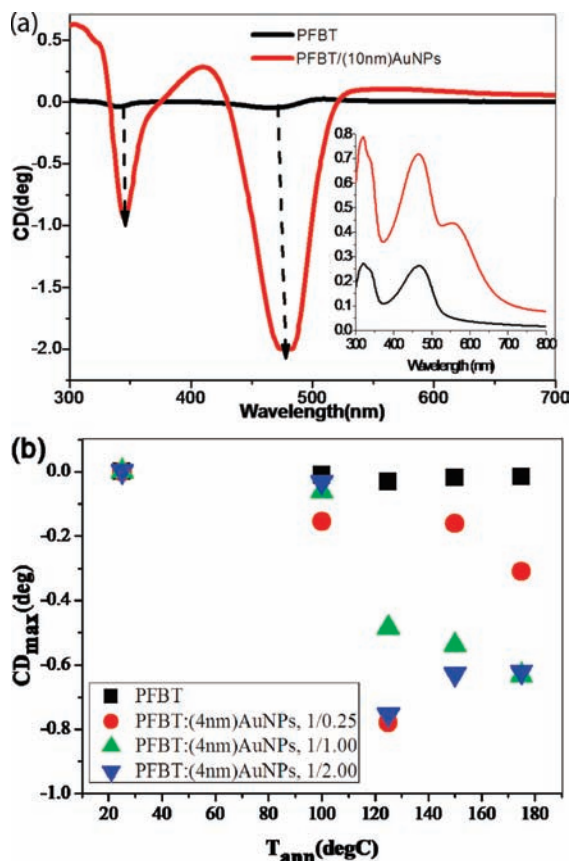
Figure 2. (a) UV−vis absorption (inset) and CD spectra of PFBT and AuNP/PFBT films annealed at 150 °C. (b) Annealing temperature dependence of maximum CD measured in thin annealed films of pure PFBT and PFBT/(4 nm)AuNP nanocomposites at three different PFBT:Au mass ratios. For both parts, identical amounts of polymer were used in each film.

(Figure 2a). In this case, which showed the largest absolute CD signal among the films studied, the maximum CD signal from the nanocomposite was 1500 times that of a pure nonannealed polymer film. The nonannealed nanocomposite had a maximum CD signal just twice that of the nonannealed pure polymer film. While annealing led to a 48-fold increase in the maximum CD of the pure polymer, it led to more than a 700-fold increase in the maximum CD of the nanocomposite. When smaller (~4 nm) AuNPs were used, annealing not only increased the intensity of the surface plasmon absorbance band but also led to a red shift in the CD bands (Figure S4). AFM and SEM analysis suggest that this results from aggregation and sintering of the particles. The close proximity of AuNPs in aggregates induces coupling of their plasmon oscillations, resulting in a red shift in the absorption band that depends mainly on the interparticle distance and orientation.[25]

A clear change in the spectrum was apparent when polymer/AuNP composites with several different ratios of PFBT to (4 nm)AuNPs were compared (Figure 2b). Composites with a 1/0.25 PFBT/AuNP mass ratio developed their maximum CD signal within a few minutes of annealing. The highest CD intensity was observed for annealing at 125 °C, which was also the case for the pure PFBT. At higher temperatures a steady decline was observed. The increase of CD was clearly slower for the (1/2) composite, which reached its maximum value after 15 min of annealing, but again the maximum CD was obtained at 125 °C. In contrast, the (1/1) composite continued to show a slight increase in CD intensity at higher temperatures (150 and 175 °C). Thus, it is clear that the helical ordering that takes place during annealing occurs more

slowly with increased AuNP content. It is not surprising that the addition of relatively immobile AuNPs should slow the dynamics of polymer rearrangement and helical assembly. The reduction in CD at high temperature may be due to chemical decomposition of the polymer or a slow transition to a state with less helical ordering. While the AuNPs may affect the rate of this decrease, it occurs even in their absence and thus cannot be attributed purely to AuNP sintering or aggregation. For (10 nm)AuNP/PFBT nanocomposites, the maximum CD was generally obtained at the highest annealing temperature (175 °C) (Figures S5, S6). The need for a higher annealing temperature is consistent with the larger AuNPs impeding helical assembly of the PFBT to a greater degree than the smaller particles, simply because they have lower mobility. In addition, the maximum enhancement of CD intensity by annealing was greater for the smaller AuNPs than for the larger ones.

Similar to pure chiral PFBT,[23] the increase in CD intensity with film thickness was superlinear (Figure S7). This suggests that similar structural features are responsible for the observed CD effects in the nanocomposites as in pure chiral PFBT. Furthermore, a chiral arrangement of the nanoparticles leading to the plasmon-coupled CD response in the vicinity of the plasmonic frequency would also predict such a thickness dependence of CD intensity. Thus, the enhanced optical activity can be related to three mechanisms: (i) supramolecular ordering, (ii) plasmonic coupling between helically arranged Au NPs because of this supramolecular ordering,[26a] and (iii) dipole−dipole exciton-plasmon coupling resulting in transfer of chirality to individual Au NPs.[26b] According to Govorov et al.[26b] the third mechanism can contribute significantly if NPs of larger size, between 20 and 40 nm, are used, which may be the case if NPs aggregate at higher annealing temperatures. Quantifying the individual contributions of each of these three mechanisms to an overall CD response is difficult because they spectrally overlap. However, we observe that (i) supramolecular organization during annealing produced a much greater CD enhancement for the nanocomposites than for the pure polymer; (ii) the highest CD response of the AuNP/PFBT composite was obtained at an annealing temperature below the aggregation threshold; and (iii) CD enhancement by AuNPs before annealing (2-fold) was much smaller than that after annealing (more than 700-fold). These observations suggest that plasmonic enhancement of chirality due to helical arrangement of Au NPs is the main mechanism leading to the large CD. The conformational stability of foldamers has been shown to lead to an amplification of chirality in solution.[27] Thus, an alternative mechanism for enhancement in chirality could be increased helical ordering induced by the gold NPs. However, if NP stabilization of helical conformation led to the observed effect, similar enhancement should be achieved using dielectric NPs, which are not coupled electromagnetically to the chiral polymer. To further clarify the mechanism of chirality enhancement we repeated the experiment with ZnO nanoparticles in place of the gold nanoparticles. In this case, excitonic coupling between NPs and the $\pi-\pi^*$ band of PFBT is greatly reduced, because the ZnO NPs do not absorb at visible wavelengths. With ZnO NPs, no significant CD enhancement was observed (Figure S8). This strongly suggests that the CD enhancement is dependent upon the electronic coupling between the NPs and PFBT. SEM and AFM imaging provides direct evidence of helical ordering in both the pure PFBT and the nanocomposites. Tapping-mode AFM images of spin-coated films (Figure S10) showed that the surface height variation increased somewhat after annealing at or above 125 °C. More commonly, polymer films become smoother after annealing. In the present case, this increased height variation appears to result from the formation of helical fibrils. Such fibrils are clearly visible in SEM images
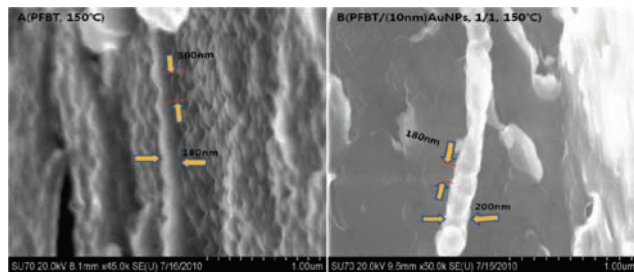
Figure 3. SEM images of (a) pure PFBT and (b) AuNP/PFBT nanocomposite at film edges, showing helical fibrils.
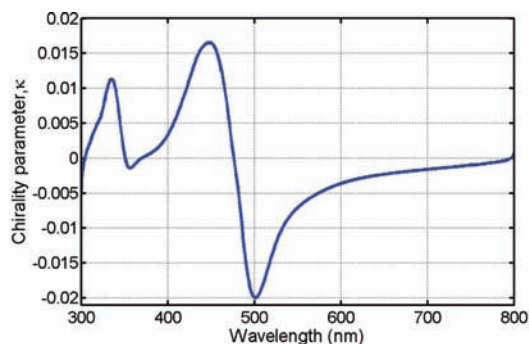

Figure 4. Spectrum of chirality parameter of the PFBT/AuNPs composite from analysis of the CD spectrum of Figure 2a.

(Figure 3) at breaks in the film or near edges, where the internal structure of the film was visible.

Finally, to extract the absolute optical activity of our composite material we obtained the dispersion of the chirality parameter, $\kappa = 3\phi c/\omega(n^2 + 2)$, where ϕ is the optical rotation, through Kramers−Kronig transformation of the measured ellipticity (CD) spectrum (Figures S13 and 4).[26] The film thickness of 100 nm used in these calculations was based on SEM (Figure S12), AFM, and reflectance measurements. The chirality parameter reached a maximum value of −0.02 at 500 nm. Thus, the chirality parameter of the PFBT/AuNP nanocomposite dramatically exceeds that of all of the previously known organic and metallo-organic structures. A combination of enhancement mechanisms, dominated by helical ordering of the AuNPs, is responsible for this extremely large optical chirality parameter.

Supporting Information Available: Further details of experimental procedure; NMR, GPC, and DSC characterization of the polymer (PFBT); UV−visible and CD spectra; transmission electron microscopy (TEM); Atomic force microscopy (AFM); Scanning electron microscopy (SEM); Spectra of refractive index derived from transmission and reflection measurements. This material is available free of charge via the Internet at http://pubs.acs.org.

References

(1) Scherf, U.; List, E. J. W. *Adv. Mater.* **2002**, *14*, 477.
(2) Neher, D. *Macromol. Rapid Commun.* **2001**, *22*, 1365.
(3) Bernius, M. T.; Inbasekaran, M.; O'Brien, J.; Wu, W. *Adv. Mater.* **2000**, *12*, 1737.
(4) Inbasekaran, M.; Woo, E.; Wu, W.; Bernius, M.; Wujkowski, L. *Synth. Met.* **2000**, *397*, 111.
(5) Wang, X.; Perzon, E.; Mammo, W.; Oswald, F.; Admassie, S.; Persson, N.-K.; Langa, F.; Andersson, M. R.; Inganäs, O. *Thin Solid Films* **2006**, *576*, 511–512.
(6) Kim, Y.; Cook, S.; Choulis, S. A.; Nelson, J.; Durrant, J. R.; Bradley, D. D. C. *Chem. Mater.* **2004**, *16*, 4812.
(7) Kietzke, T.; Neher, D.; Kumke, M.; Montenegro, R.; Landfester, K.; Scherf, U. *Macromolecules* **2004**, *37*, 4882.
(8) Snaith, H. J.; Arias, A. C.; Morteani, A. C.; Silva, C.; Friend, R. H. *Nano Lett.* **2002**, *2*, 1353.
(9) Grice, A. W.; Bradley, D. D. C.; Bernius, M. T.; Inbasekaran, M.; Wu, W. W.; Woo, E. P. *Appl. Phys. Lett.* **1998**, *73*, 629.
(10) He, Y.; Gong, S.; Hattori, R.; Kanicki, J. *Appl. Phys. Lett.* **1999**, *74*, 2265.
(11) Voigt, M.; Chappell, J.; Rowson, T.; Cadby, A. J.; Geoghegan, M.; Jones, R. A. L.; Lidzey, D. G. *Org. Electron.* **2005**, *6*, 35.
(12) Lee, J.; Jung, B.-J.; Lee, S. K.; Lee, J.-I.; Cho, H.-J.; Shim, H.-K. *J. Polym. Sci. A: Polym. Chem.* **2005**, *43*, 1845.
(13) Wu, W.-C.; Liu, C.-L.; Chen, W.-C. *Polymer* **2006**, *47*, 527.
(14) (a) Baiker, A. *J. Mol. Catal. A: Chem.* **1997**, *115*, 473. (b) Wells, P. B.; Wilkinson, A. G. *Top. Catal.* **1998**, *5*, 39. (c) Augustine, R. L.; Tanielyan, S. K.; Doyle, L. K. *Tetrahedron: Asymmetry* **1993**, *4*, 1803. (d) Margitfalvi, J. L.; Tálas, E.; Tfirst, E.; Kumar, C. V.; Gergely, A. *Appl. Catal. A: Gen.* **2000**, *191*, 177. (e) Zaera, F. *J. Phys. Chem. B* **2002**, *106*, 4043. (f) LeBlanc, R. J.; Chu, W.; Williams, C. T. *J. Mol. Catal. A: Chem.* **2004**, *212*, 277. (g) Chu, W.; LeBlanc, R. J.; Williams, C. T.; Kubota, J.; Zaera, F. *J. Phys. Chem. B* **2003**, *107*, 14365.
(15) (a) Hazen, R. M.; Sholl, D. S. *Nat. Mater.* **2003**, *2*, 367. (b) Horvath, J. D.; Koritnik, A.; Kamakoti, P.; Sholl, D. S.; Gellman, A. J. *J. Am. Chem. Soc.* **2004**, *126*, 14988. (c) Horvath, J. D.; Gellman, A. J. *J. Am. Chem. Soc.* **2002**, *124*, 2384.
(16) Wei, J. J.; Schafmeister, C.; Bird, G.; Paul, A.; Naaman, R.; Waldeck, D. H. *J. Phys. Chem. B* **2006**, *110*, 1301.
(17) Baev, A.; Samoc, M.; Prasad, P. N.; Krykunov, M.; Autschbach, J. *Optics Express* **2007**, *15*, 5730.
(18) (a) Tretyakov, S.; Sihvola, A.; Jylhä, L. *Photonics and Nanostructures - Fundamentals and Applications* **2005**, *3*, 107–115. (b) Rockstuhl, C.; Lederer, F.; Etrich, C.; Pertsch, T.; Scharf, T. *Phys. Rev. Lett.* **2007**, *99*, 017401.
(19) (a) Schaaff, T. G.; Knight, G.; Shafigullin, M. N.; Borkman, R. F.; Whetten, R. L. *J. Phys. Chem. B* **1998**, *102*, 10643. (b) Schaaff, T. G.; Whetten, R. L. *J. Phys. Chem. B* **2000**, *104*, 2630. (c) Yao, H.; Miki, K.; Nishida, N.; Sasaki, A.; Kimura, K. *J. Am. Chem. Soc.* **2005**, *127*, 15536.
(20) (a) Lieberman, I.; Shemer, G.; Fried, T.; Kosower, E. M.; Markovich, G. *Angew. Chem., Int. Ed.* **2008**, *47*, 4855. (b) Elliott, S. D.; Moloney, M. P.; Gun'ko, Y. K. *Nano Lett.* **2008**, *8*, 2452. (c) Nakashima, T.; Kobayashi, Y.; Kawai, T. *J. Am. Chem. Soc.* **2009**, *131*, 10342.
(21) (a) Roman-Velazquez, C. E.; Noguez, C.; Garzon, I. L. *J. Phys. Chem. B* **2003**, *107*, 12035. (b) Tang, Z. Y.; Wang, Y.; Giersig, M.; Kotov, N. A. *J. Am. Chem. Soc.* **2006**, *128*, 6730. (c) Li, T. H.; Park, H. G.; Lee, H. S.; Choi, S. H. *Nanotechnology* **2004**, *15*, S660. (d) Gautier, C.; B″urgi, T. *J. Am. Chem. Soc.* **2006**, *128*, 11079. (e) Ha, J.-M.; Solovyov, A.; Katz, A. *Langmuir* **2009**, *25*, 153.
(22) (a) Shemer, G.; Krichevski, O.; Markovich, G.; Molotsky, T.; Lubitz, I.; Kotlyar, A. B. *J. Am. Chem. Soc.* **2006**, *128*, 11006. (b) George, J.; Thomas, K. G. *J. Am. Chem. Soc.* **2010**, *132*, 2502.
(23) Abbel, R.; Schenning, A. P. H. J.; Meijer, E. W. *Macromolecules* **2008**, *41*, 7497.
(24) (a) Yong, K.-T.; Sahoo, Y.; Choudhury, K. R.; Swihart, M. T.; Minter, J. R.; Prasad, P. N. *Chem. Mater.* **2006**, *18*, 5965. (b) Hiramatsu, H.; Osterloh, F. E. *Chem. Mater.* **2004**, *16*, 2509.
(25) (a) Jain, P. K.; Huang, W. Y.; El-Sayed, M. A. *Nano Lett.* **2007**, *7*, 2080. (b) Joseph, S. T. S.; Ipe, B. I.; Pramod, P.; Thomas, K. G. *J. Phys. Chem. B* **2006**, *110*, 150. (c) Padmanabhan, P.; Thomas, K. G. *Adv. Mater.* **2008**, *20*, 4300. (d) Bakr, O. M.; Wunsch, B. H.; Stellacci, F. *Chem. Mater.* **2006**, *18*, 3297.
(26) (a) Fan, Z.; Govorov, A. O. *Nano Lett.* **2010**, *10*, 2580. (b) Govorov, A. O.; Fan, Z.; Hernandez, P.; Slocik, J. M.; Naik, R. R. *Nano Lett.* **2010**, *10*, 1374.
(27) Rivera-Fuentes, P.; Alonso-Gomez, J. L.; Petrovic, A. G.; Santoro, F.; Harada, N.; Berova, N.; Diederich, F. *Angew. Chem., Int. Ed.* **2010**, *49*, 2247.

JA107064A